ACS SyntheticBiology

pubs.acs.org/synthbio

Research Article

Mechanistic Insights into Cell-Free Gene Expression through an Integrated -Omics Analysis of Extract Processing Methods

Blake J. Rasor,[▽] Payal Chirania,[▽] Grant A. Rybnicky,[▽] Richard J. Giannone, Nancy L. Engle, Timothy J. Tschaplinski, Ashty S. Karim, Robert L. Hettich,* and Michael C. Jewett*

Cite This: *ACS Synth. Biol.* 2023, 12, 405−418

Read Online

ACCESS | Metrics & More | Article Recommendations | Supporting Information

ABSTRACT: Cell-free systems derived from crude cell extracts have developed into tools for gene expression, with applications in prototyping, biosensing, and protein production. Key to the development of these systems is optimization of cell extract preparation methods. However, the applied nature of these optimizations often limits investigation into the complex nature of the extracts themselves, which contain thousands of proteins and reaction networks with hundreds of metabolites. Here, we sought to uncover the black box of proteins and metabolites in *Escherichia coli* cell-free reactions based on different extract preparation methods. We assess changes in transcription and translation activity from σ^{70} promoters in extracts prepared with acetate or glutamate buffer and the common post-lysis processing steps of a runoff incubation and dialysis. We then utilize proteomic and metabolomic analyses to uncover potential mechanisms behind these changes in gene expression, highlighting the impact of cold shock-like proteins and the role of buffer composition.

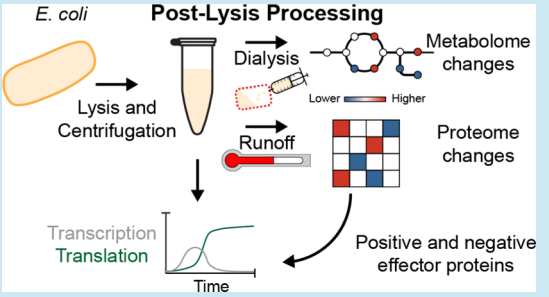

KEYWORDS: *cell-free protein synthesis, in vitro, TX-TL, proteomics, metabolomics*

INTRODUCTION

Cell-free systems composed of crude cell extracts in the absence of cell viability, replication, and membrane barrier constraints[1−3] enable the study of biological processes,[4−7] synthesis of therapeutics,[8−12] biosensing and transcriptional cascades,[13−19] genetic part prototyping,[20−24] and biochemical production.[25−31] *Escherichia coli* extracts serve as the most common platform for cell-free systems with strains extensively optimized for diverse applications incorporating cell-free gene expression (CFE), such as A19 and BL21 for protein synthesis,[32,33] CLM24 for glycosylation,[34] SHuffle for disulfide bonded products,[35] and C321.ΔA.759 for noncanonical amino acid incorporation.[36,37] In fact, methods for generating *E. coli* extracts have shaped contemporary approaches following the same general protocol regardless of the source species. Cells are typically grown in rich media to a mid-exponential phase[38,39] or in defined media for high density growth[40,41] and harvested in acetate or glutamate buffers.[42,43] Biomass is lysed through physical or chemical means, and the cell lysate is centrifuged to remove cell debris and isolate important CFE components including enzymes, translation machinery, and membrane vesicles formed during lysis.[33,39,44,45] Then, the extract can be processed through incubation (referred to historically as a runoff reaction) and/or dialysis.[44]

Post-lysis processing steps such as runoff incubation and dialysis depend both on the strain and the desired application. For example, runoff and dialysis tend to increase CFE from viral promoters (e.g., T7 promoter) for K-strain derivatives,[38] while these processing steps are necessary for robust expression from endogenous *E. coli* promoters, such as σ^{70}-based promoters, in B-strain derivatives.[46,47] The "runoff" step is an incubation after lysis that is hypothesized to allow ribosomes to finish translating endogenous mRNA until transcripts degrade, and the subsequent dialysis removes accumulated metabolites.[44,46] Some strains require these processing steps for sufficient gene expression, whereas other strains (even of the same species) may lose in vitro activity after runoff and dialysis.[39,44] In most cases, extract processing and reaction composition are optimized for end-point protein synthesis yields or metabolic activity with minimal assessment of systemic changes.[33,38,48] Although washing and processing steps may be altered for efficiency[32] and some reaction components may be substituted to reduce the overall cost of CFE,[49] most studies follow time-tested protocols to maximize expression yields and intra-lab consistency.[50] The focus on gene expression yields has minimized the exploration of the underlying biochemical changes in cell extracts that result from variables during cell growth, washing/harvesting, lysis, incubation, dialysis, and CFE reaction conditions.

Received: June 28, 2022
Published: January 26, 2023

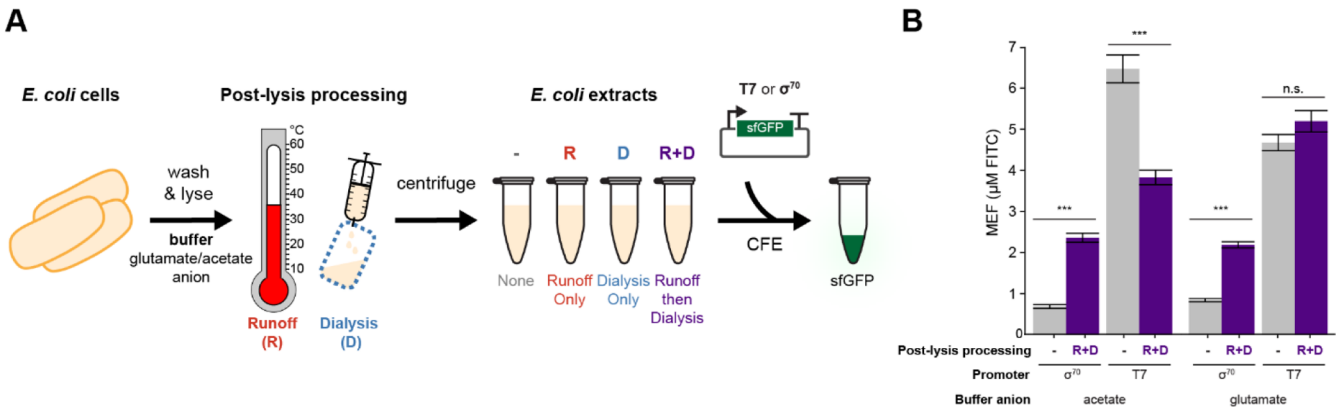

Figure 1. Post-lysis processing has a significant effect on CFE. (A) Schematic of *E. coli* extract preparation, including no post-lysis processing, a runoff incubation for 80 min at 37 °C (R), dialysis for 3 h at 4 °C (D), or runoff and dialysis in sequence (R + D). Differentially processed extracts were combined with CFE reagents and expression templates for sfGFP with either σ^{70} or T7 promoters at 5 nM. (B) Comparing CFE reactions using extracts with no post-lysis processing to those with runoff + dialysis reveals a significant increase in σ^{70} expression after processing, regardless of the buffer salt used during extract preparation. T7 expression is not impacted by processing glutamate-based extracts, but T7 yields are decreased by processing in acetate-based extracts. Data represent mean ± standard error of the mean of four biological replicates with four technical replicates each.

Elucidating the complex, multicomponent interactions in *E. coli* cell extracts requires in-depth and untargeted analytical methods, such as metabolomics and proteomics.[51] To this end, several studies have incorporated -omics analyses to catalogue the contents of the *E. coli* extract,[52,53] assess extract changes due to culture medium formulation and cell stress,[41,54−56] and monitor CFE with greater resolution.[53,57] While these efforts have provided insights into the extract composition under specific circumstances, the biochemical impacts of common post-lysis processing steps (including centrifugation, runoff, and dialysis) remain unresolved. The lack of a deeper understanding stems in part from the analysis of runoff and dialysis in tandem using gene expression as the measured readout,[46,54,58] although some streamlined protocols have omitted dialysis to reduce extract preparation time.[59,60] Understanding how each post-lysis processing step affects the proteome, metabolome, and activity of cell extracts could expand opportunities to optimize and tailor CFE systems for specific applications.

In this work, we sought to characterize the behavior and composition of *E. coli* extracts prepared by following different post-lysis processing steps to better understand the biochemical changes caused by extract processing. First, we assessed the impact of buffer salts and processing steps (separately and together) on transcription and translation kinetics. Next, we used gas chromatography−mass spectrometry (GC−MS) to determine the identity and relative abundances of metabolites in each of the extract samples. Simultaneously, we used liquid chromatography with tandem mass spectrometry (LC−MS/MS) to determine the identity and relative abundances of proteins in cell lysate before centrifugation and in clarified extracts with no processing, runoff, dialysis, or both additional steps. After observing that the most significant impact of extract processing correlated with changes in proteome composition, we identified key proteins facilitating endogenous σ^{70}-based expression by assessing transcription and translation in processed extracts after supplementation of the most significantly decreased proteins. We anticipate that understanding the proteomic and metabolomic changes that occur during each step of *E. coli* extract preparation and processing will allow for enhanced optimization of and insights into this platform's growing repertoire of applications.

RESULTS AND DISCUSSION

Post-Lysis Processing Increases CFE from σ^{70} Promoters. First, we sought to assess the effects of post-lysis processing on combined transcription and translation in *E. coli* BL21 extracts. To achieve this, we produced extracts with no further processing and extracts that were incubated for an 80 min runoff reaction at 37 °C, followed by dialysis for 3 h at 4 °C (Figure 1A). We prepared and processed these extracts individually using acetate or glutamate buffer salts to investigate whether there is a basis for the use of acetate buffer for T7-based expression applications and the use of glutamate buffer for endogenous polymerase-based expression applications.[37,48,61,62] To assess CFE systems with both endogenous (typically used in genetic circuit applications) and exogenous gene expression (typically used for protein biosynthesis and enzyme prototyping), we compared the CFE of super-folder green fluorescent protein (sfGFP) transcribed from σ^{70} and T7 promoters and observed that post-lysis processing increased σ^{70} promoter expression ∼3-fold in both buffer conditions (Figure 1B). However, while T7 expression in glutamate buffer remained comparable with or without post-lysis processing, T7 expression in acetate buffer decreased after processing (Figure 1B). These results are consistent with previous studies.[38,46] Notably, the kinetic traces of combined transcription and translation differed between the two promoters based on the post-lysis processing treatment. While T7 expression produced sfGFP at approximately the same rate in CFE reactions from extracts with and without post-lysis processing, the rate of sfGFP production from the σ^{70} promoter was increased at least 3-fold after runoff and dialysis (Figure S1).

We next investigated the impact of each post-lysis processing step on transcription and translation driven by a σ^{70} promoter, which is important for the implementation of complex genetic programs incorporating bacterial transcription factors[14] and other genetic circuits.[47] We first compared the kinetic profiles of sfGFP expression from combined transcription and translation under control of σ^{70} promoters. We titrated 1−20

https://doi.org/10.1021/acssynbio.2c00339
ACS Synth. Biol. 2023, 12, 405−418

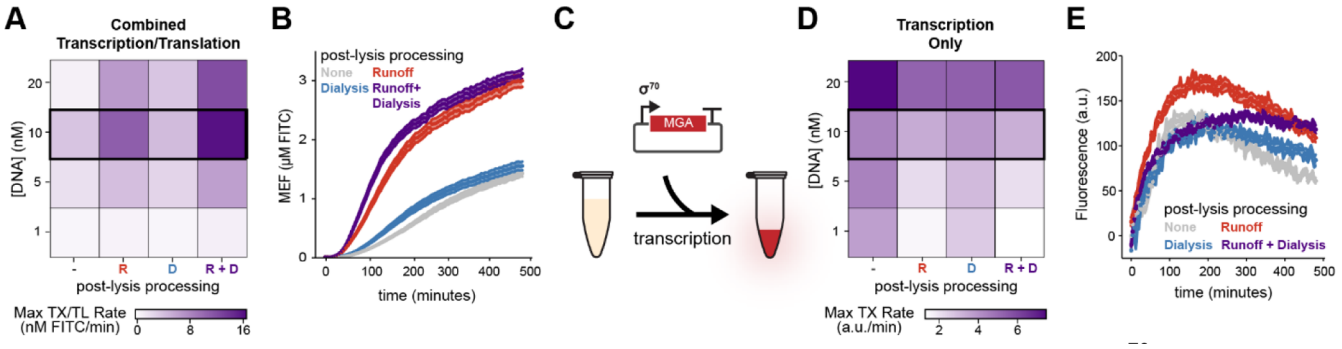

Figure 2. Runoff incubation accounts for most of the observed increase in σ^{70} expression. Cell-free expression reactions were incubated at 30 °C with plasmids in extracts with no processing (gray), with runoff (red), with dialysis (blue), and with both runoff and dialysis (purple). (A) Initial transcription/translation rates were calculated from reactions with 1, 5, 10, and 20 nM σ^{70}-sfGFP plasmid and showed increased expression rates in extracts with runoff. (B) Kinetic measurements of sfGFP expression with 10 nM σ^{70}-sfGFP plasmid illustrate a shift in transcription/translation rates after dialysis with runoff, driving the majority of the increase in expression over unprocessed extracts. (C) Schematic of transcription-only reactions with expression plasmids for MGA driven by a σ^{70} promoter. (D) Initial transcription rates were calculated from reactions with 1, 5, 10, and 20 nM MGA plasmid and indicate greater transcriptional limitation after runoff and similar transcription rates after dialysis relative to the unprocessed extract. (E) Kinetics of transcription with 10 nM DNA reveals greater MGA production after runoff alone. Kinetic curves for other DNA concentrations are presented in Figures S2 snd S3. Data represent mean ± standard error of the mean of four biological replicates with four technical replicates each.

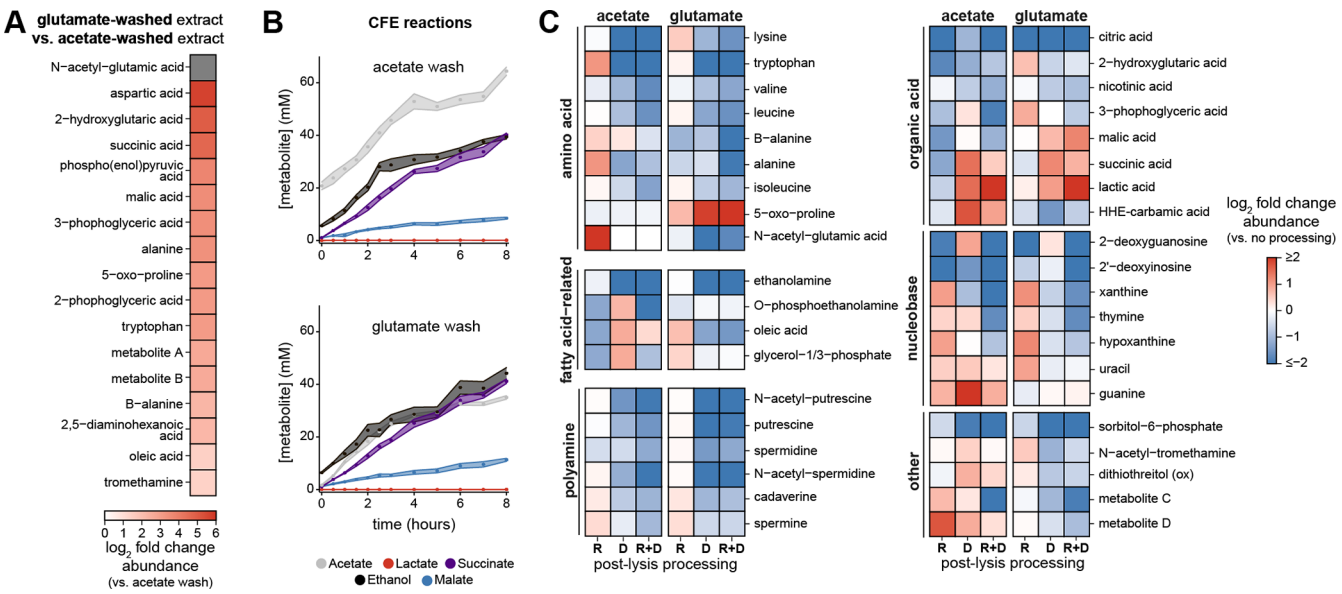

Figure 3. Dialysis and wash buffer alter the extract metabolome, but the reaction composition shapes metabolism during CFE. (A) Heat map of metabolites significantly more abundant in glutamate-washed extracts than those prepared with acetate buffer. *N*-acetyl-glutamic acid was only detected in glutamate-based extracts. (B) Targeted metabolite measurements in CFE reactions containing extracts processed with runoff + dialysis in acetate or glutamate buffer. Data represent mean ± standard deviation of four biological replicates with separate reactions measured at each time point. (C) Changes in metabolite abundance are shown for differentially processed extracts relative to the unprocessed extract prepared with the same buffer salt. N-[2-hydroxy-1,1-bis(hydroxymethyl)-ethyl]-carbamic acid (abbreviated HHE-carbamic acid) is a modified metabolite from the culture media. Data indicate the $\log_2$ fold change of metabolite abundance in cell extracts prepared from four biological replicates. Information about unknown metabolites is included in Table S1.

nM concentrations of σ^{70}-sfGFP and observed changes in the maximum apparent translation rate in each extract (Figure 2A). Maximum rates were determined by linear regression over a sliding window of 20 minute intervals to identify the greatest slope. From these data, we observed that runoff alone is sufficient to maintain the maximum translation yield of sfGFP with dialysis after runoff, providing a further increase in the apparent translation rate (Figure S2). Comparing the expression kinetic profiles of reactions with 10 nM DNA highlights the impact of runoff alone in increasing σ^{70}-sfGFP production, while dialyzing the extracts increases the initial expression rate (Figure 2B). We further assessed transcriptional limitations by titrating a σ^{70}-controlled malachite green aptamer (MGA) RNA, which interacts with the malachite green dye to produce a fluorescence signal (Figures 2C−E and S3). The σ^{70}-MGA plasmid was titrated from 1−20 nM in CFE reactions to observe changes in the maximum transcription rate in each extract (Figure 2D). The unprocessed extract shows no transcriptional limitation up to 10 nM plasmid, with an increased transcription rate only occurring with 20 nM DNA. However, runoff incubation of extracts appears to impose a transcriptional limitation, requiring higher DNA

https://doi.org/10.1021/acssynbio.2c00339
ACS Synth. Biol. 2023, 12, 405−418

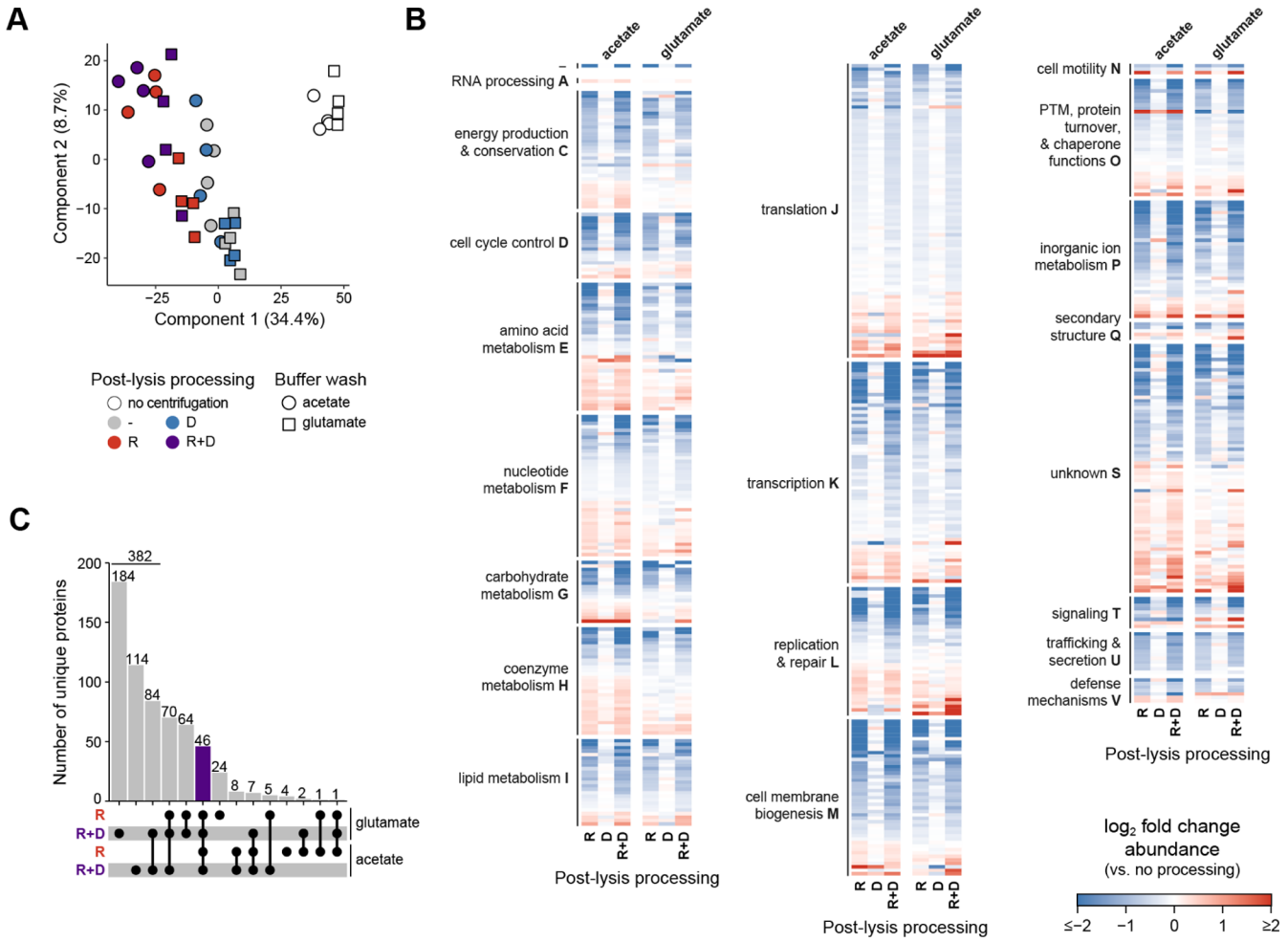

Figure 4. Post-lysis centrifugation and runoff significantly alter the extract proteome. (A) Principal component analysis of cell lysates prior to centrifugation and differentially processed extracts indicates significant proteomic changes from the initial centrifugation (converting the lysate into the extract) and runoff. (B) Heat map showing the $\log_2$(fold change) abundance changes in significant proteins in the processed extracts relative to the unprocessed extracts for the respective salts. Average $\log_2$(fold change) of cell extracts prepared from four biological replicates is shown and grouped by COG annotations. Coarse groupings of COG designations are transcription/translation (A, J, K, and O), cell maintenance (D, L, M, N Q, T, U, and V), metabolism (C, E, F, G, H, I, and P), and unknown (-, S). (C) Upset plot showing the number of significantly depleted proteins in each extract processed using runoff incubation, highlighting 46 proteins commonly depleted across all conditions with runoff.

concentrations to improve transcription rates. Despite this, comparing the kinetic profiles of transcription with 10 nM DNA indicates that extracts processed with runoff alone display greater MGA fluorescence after 1 h (Figure 2E). This suggests an increase in RNA stability after runoff (Figure S3).

Our data indicate that the primary limitation to σ^{70} expression pertains to translation and that runoff incubation reduces this limitation. Although our previous study saw that combined runoff and dialysis increased transcription from both T7 and σ^{70} promoters, we did not observe this phenomenon here.[46] Key differences between our work and these prior experiments are the chassis strain and lysis method employed. Silverman et al. used the extract from Rosetta2 cells (carrying the pRARE plasmid for tRNA expression) prepared by sonication, while we used BL21 Star (DE3) (which has a truncated version of RNase E) prepared by homogenization. This could result in differential transcription kinetics, RNA stability, or other factors related to our observation of MGA expression, which emphasizes the importance of chassis strain selection for the desired cell-free application.[44,46] The RNase E truncation product also decreases in abundance after runoff, which may further reduce the activity of this enzyme (Data Set S2). However, translational limitation during CFE from both viral and endogenous promoters is supported by several studies that incorporated ribosome profiling,[63] LC−MS,[55,64] and quantitative modeling.[65−67]

Dialysis and Endogenous Metabolism Alter the Extract Metabolome. The observed transcriptional and translational changes across extracts with dialysis suggest that small molecule metabolite and cofactor differences could underpin the impact of this post-lysis processing step on CFE.[46] We first investigated metabolic differences via GC−MS in extracts alone (not CFE reactions) produced using glutamate and acetate buffers, expecting different profiles due to *E. coli*'s ability to utilize both acetate and glutamate as carbon sources via AckA/Pta and GhdA, respectively. We found that in unprocessed extracts, the primary metabolic differences are related to the glutamate metabolism, with glutamate derivatives such as aspartic acid and succinic acid over 20-fold more abundant in glutamate-based extracts than in acetate-based extracts (Figure 3A). Targeted measurements of central metabolites via high-performance liquid chromatog-

https://doi.org/10.1021/acssynbio.2c00339
ACS Synth. Biol. 2023, 12, 405−418

raphy (HPLC) show higher succinate and ethanol concentrations for glutamate-based extracts, likely from glutamate entering the tricarboxylic acid cycle via α-ketoglutarate, while lactic acid is not observed (Figure S4). These metabolites are depleted after dialysis, although acetate concentrations remain high as expected for extracts dialyzed into acetate buffers. In addition, using extracts processed with runoff and dialysis in 8 h CFE reactions show few differences in metabolic profiles over time whether glutamate or acetate salts are used in the wash buffer (Figure 3B), suggesting that extract processing plays a more significant role than buffer composition in the observed shift in gene expression profiles.

We next measured metabolite abundances in each processed extract and compared these measurements to the abundances in the corresponding unprocessed extract prepared with the same buffer (i.e., extracts were grouped based on the use of acetate or glutamate buffers during preparation). Of the metabolites that were detected by this method, 40 compounds were present at significantly different concentrations after one or more post-lysis processing steps (Figure 3C and Data Set S1). Generally, amino acids (aside from 5-oxo-proline derived from glutamate), citric and nicotinic acids, sorbitol-6-phosphate, and polyamines are depleted by dialysis in both buffer salt conditions (Figure 3C). Further, lysine, tryptophan, ethanolamine, citric acid, sorbitol-6-phosphate, putrescine, and N-acetyl-spermidine are depleted at least 2-fold after dialysis. Additionally, most of the detected nucleobases are significantly depleted only after the combination of runoff and dialysis. Note that lactic acid was not observed by HPLC due to the higher limit of detection relative to GC−MS (Figure S4).

Our targeted and untargeted metabolic analyses indicate that CFE formulations more significantly impact metabolic flux than extract processing due to the high concentrations of exogenous salts (primarily glutamate), carbon/energy sources, and other molecules.[54] This is highlighted by the fact that many of the metabolites that decrease in the extract during post-lysis processing (including amino acids, nucleobases, and polyamines) are added to CFE reactions in most formulations.[62] However, the presence of high concentrations of acetate or glutamate anions in the wash buffer during cell harvesting does impact the underlying metabolome of resulting cell extracts and could alter the proteome and observed gene expression activity through regulatory changes that occur prior to cell lysis, particularly during the runoff incubation.[62,68] Concentrations of CFE reagents and their byproducts must also be considered and optimized for different applications.[62] For example, including polyamines (such as putrescine) and crowding reagents (such as polyethylene glycol and Ficoll) can improve CFE through nucleic interactions and/or molecular crowding effects, but these components can reduce protein synthesis above an optimal concentration.[54,66,69] In addition to these insights, the metabolomics data enable inferences into related compounds that could not be detected on this specific analytic pipeline, such as some phosphorylated metabolites.

Initial Centrifugation and Runoff Lead to Shifts in the Extract Proteome. Beyond metabolomics, we hypothesized that post-lysis processing impacts the distribution of proteins in extracts and in turn CFE activity. To test this hypothesis, we used LC−MS/MS to analyze cell lysates and extracts using differential processing. We quantified 1892 high-quality proteins across all the samples, covering 45.5% of the *E. coli* genome (Data Set S2). We found that cell lysates prior to centrifugation cluster separately from all clarified extract samples in the proteome space (Figure 4A). This separation is influenced by both the composition (the number of quantified proteins) (Figure S5) and abundance of specific proteins (Figure S6), which we found to be significantly different (e.g., expected depletion of membrane proteins) in the cell lysates prior to centrifugation compared to the resulting extracts after centrifugation. In addition, extracts subjected to runoff cluster together and differ from extracts with no post-lysis processing or with dialysis alone irrespective of the buffer used (Figure 4A). Interestingly, more membrane proteins were identified here in extracts from *E. coli* BL21 Star (DE3) than in extracts from *E. coli* A19 or BL21Rosetta2 analyzed in previous cell-free proteomics studies,[52,53] which could be due to differences in the source strain, lysis, centrifugation, and post-lysis processing conditions, or employed mass spectrometric methods. A recent comparison of lysis and centrifugation methods indicated that homogenization (the lysis method employed here) results in a higher concentration of membrane vesicles in extract than sonication, and centrifugation at 12,000*g* rather than the traditional 30,000*g* increases vesicle concentration by up to 2-fold.[45]

Next, we characterized the impact of post-lysis processing on the extract proteome by comparing the abundance of proteins in each extract to the unprocessed extract prepared with the same buffer salt categorized by the cluster of orthologous groups (COG) (Figure 4B). Of the nearly 1900 quantified proteins, 614 significantly changed in abundance (p-value < 0.05) in at least one processed extract relative to the corresponding unprocessed extract. The most significant changes in protein abundance occurred in processed extracts with runoff incubation, suggesting that runoff is primarily responsible for altering the proteome of extracts during post-lysis processing. Beyond protein abundance, we also investigated changes in protein modifications that could result from the additional processing steps and time such as oxidation. Although select proteins demonstrated enhanced modification with one or more processing steps, the global profiles of oxidation, methylation, and deamidation remained similar across all extracts (Figure S7), which indicates that changes in protein abundances were likely the primary influencers of CFE activity.

The proteins changing significantly in abundance spanned 20 different COG categories with >50% belonging to categories related to metabolism and genetic information processing. We found that 64 significant changes in protein abundance relate to transcription (COG K) and 85 significantly different proteins relate to translation (COG J). However, 72 proteins with altered abundance have unknown functions (COG S), highlighting the likelihood of complex interactions and emergent properties as the extract proteome changes with centrifugation and post-lysis processing. The depletion of metabolically related proteins (COGs C, E, F, G, H, I, and P) can provide additional insights. Reduced concentrations of enzymes and regulatory proteins (combined with the lack of genomic regulation in the cell extract) alter the metabolic profile of the cell-free system and links observed changes in the proteome and metabolome. For example, succinate accumulation correlates with depletion of succinate dehydrogenase (SDH) subunits. *E. coli* normally has ~0.5 mM succinate in the cytoplasm,[70] but CFE reactions (which are more dilute than cytoplasm) accumulate up to 40 mM succinate over 8 h (Figure 3B). Multiple SDH subunits (including cytochrome b556, SDH flavoprotein, the SDH

https://doi.org/10.1021/acssynbio.2c00339
ACS Synth. Biol. 2023, 12, 405−418

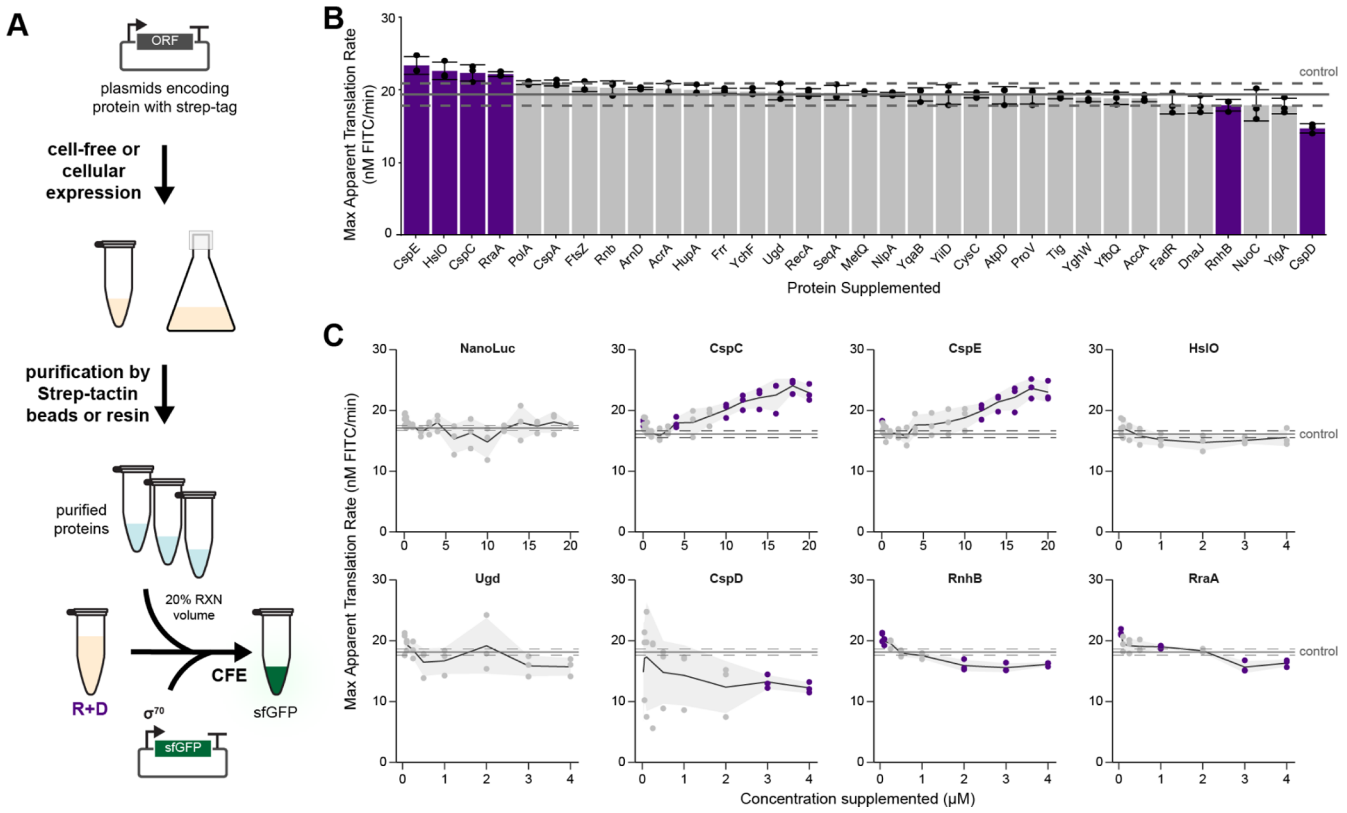

Figure 5. Supplementing depleted proteins back into CFE indicates positive and negative effectors. (A) Identified proteins were expressed by CFE or in vivo, purified, and added into CFE reactions containing the extract processed with runoff + dialysis to observe differences in the rate of σ^{70}-sfGFP expression. (B) Expression rates for reactions with supplemented proteins indicate putative effector proteins (purple) that significantly changed the expression rate ($p < 0.05$ compared to dialyzed elution buffer without the protein, indicated by a solid line ± a dashed line). (C) Effector proteins were purified at larger volumes to assess concentration-dependent impacts on sfGFP expression rates. Cold-shock proteins E and C were identified as positive effectors, while RraA, CspD, and RnhB were identified as negative effectors ($p < 0.05$, indicated in purple). Data represent mean ± standard deviation of three technical replicates.

iron−sulfur subunit, and the hydrophobic membrane anchor) decrease ∼2-fold after the initial post-lysis centrifugation and further decrease after runoff, which likely accounts for the observed decrease in enzymatic activity (Data Set S2). Connections between the proteome and metabolome of the cell extract are also evident in the literature as both biochemical profiles are impacted by the growth medium and extract preparation methods[41,54,56] and changes in enzyme concentrations alter the metabolic activity and flux.[67,71]

Although the diversity of proteins with reduced abundance after runoff highlights the complexity of analyzing cell-free systems, we wanted to identify which proteins depleted during post-lysis processing might be primary contributors to the differences observed in CFE activities. To achieve this, we found that >50% (382 out of 614 proteins) were significantly altered in extracts processed with either runoff alone (R) or when combined with dialysis (R + D) across both salt conditions (Figure 4C). However, only 46 proteins exhibited significant depletion in any extract subjected to runoff incubation, suggesting a non-random loss of these proteins due to runoff. The commonly depleted proteins spanned different COG categories and encompassed a mix of both cytoplasmic and membrane-related proteins (Table S2). These proteins included ribonucleases (RnhB and Rne), cold-shock proteins (CspD and CspE), subunit proteins from protein complexes (AcrA,B; CysA,N; FtsH,Z; HflC,K; NuoB,C; etc.), and multiple Y-proteins. To understand the potential functional relatedness of these diverse proteins, further analysis using protein interaction information from STRING revealed that the 46 common proteins are highly interconnected and have connections with 13 other proteins that were significantly depleted in one or more extracts processed with runoff (Figure S8 and Table S2). Interestingly, these additional proteins belonged to similar functional groups such as nuclease-related proteins (RnB and RrA), cold-shock proteins (CspA and CspC), and so on, which although depleted were narrowly missed by the applied significance cutoff (Table S2 and Data Set S2). The substantial interconnectedness of these 59 proteins suggests that complex interactions are involved in the observed shifts in extract activity and warranted further investigation into their role in influencing CFE activity.

Supplementing Depleted Proteins Alters Gene Expression. We wondered if the individual, putative effects on gene expression of the panel of 59 significantly depleted proteins are partially responsible for extract-specific differences in σ^{70} activity. To test this, we expressed each protein with N-terminal strep-tags via CFE using linear expression templates or in cells when soluble expression in vitro was <3.5 μM (Figure S9). Proteins were purified, desalted, and quantified (Figure S10). Next, the candidate effector proteins with >3.5 μM soluble yield were supplemented into individual CFE reactions at 20% of the final reaction volume and incubated at 30 °C for 8 h (Figure 5A). The rate of σ^{70}-sfGFP expression was measured and compared to that of control reactions

https://doi.org/10.1021/acssynbio.2c00339
ACS Synth. Biol. 2023, 12, 405−418

containing desalted elution buffer without a purified protein (Figure 5B). Kinetics and endpoint sfGFP expression for the supplementation screen are provided in Figure S11 and Table S4, respectively. Six proteins resulted in significantly increased or decreased expression rates compared to control reactions ($p < 0.05$, indicated in purple). These included cold-shock family proteins (CspC, CspD, and CspE) that are known to interact with nucleic acids,[72] a chaperone (HslO), an RNase (RnhB), and a modulator of RNase E activity (RraA). We further investigated these proteins by titrating each individually up to 4 μM in CFE reactions and measuring the rate of σ^{70}-sfGFP expression over 8 h relative to dialyzed elution buffer without a purified protein (Figure 5C), understanding that effector proteins would likely have dose-responsive impacts. We found that negative controls supplementing NanoLuc luciferase[73] and Ugd (a protein from the initial panel with no significant effect on expression) into CFE reactions exhibited no significant effect on the production of sfGFP. Importantly, each effector candidate continued to show a significant impact on CFE activity except HslO and RraA, which only enhanced CFE activity at low concentrations (Figures 5C; S10, S12, and 13 and Table S5). Given that HslO (also known as Hsp33) protects against oxidative stress[74] and we observed no global change in protein oxidation states (Figure S7), this protein may not have a significant role under the CFE conditions employed. CspC and CspE are highly expressed in cellular environments[75,76] and are among the most abundant proteins in the extract prior to runoff (Table S3), so we supplemented them up to 20 μM and found that they have significant positive effects on CFE at higher concentrations. However, CspD, RnhB, and RraA are significant negative effectors of CFE, suggesting that their depletion from the extract during runoff incubation contributes to the observed increase in σ^{70} gene expression from processed *E. coli* extracts. Although we identified both significant positive and negative protein effectors of CFE that are depleted during runoff, the observed net benefit of post-lysis processing suggests that depleting the negative effectors and interacting proteins outweighs the depletion of positive effectors, especially as the latter are present at high levels. To assess these potential interactions, the identified cold-shock family proteins were then supplemented in pairs to CFE reactions (Figure S14). The positive effectors (CspA, CspC, and CspE) at 20 μM all compensated for the negative impact of CspD at 5 μM. Additionally, CspC paired with either CspA or CspE at 15 μM increases sfGFP expression rates more than any of the positive effectors alone, suggesting synergistic effects rather than redundant mechanisms.

While complex, multicomponent interactions likely shape the overall changes in extract activity observed using post-lysis processing, the individual components highlighted in our supplementation assay provide useful insights. All the negative effectors identified here have documented interactions with RNA, providing potential mechanisms behind their observed impact on CFE rates. For example, in vivo, CspD is upregulated during the stationary phase to slow DNA replication, but it interacts with single-stranded RNA as well as DNA[77] and is regulated by Lon protease.[78] The lack of Lon protease in BL21 could make extracts from this strain more sensitive to CspD concentration. Separately, the abundance of cold-shock family proteins in this list of effector proteins is noteworthy. CspA, CspC, and CspE were previously shown to improve CFE yields with a particular impact at temperatures below 30 °C, while CspD and other cold-shock family proteins reduced the expression.[79] However, the concentration of these proteins is a key consideration. Multiple studies indicate an optimum or a plateau for the positive impact of CspA and CspE on CFE with a significant inhibitory effect at high concentrations.[79−81] With further optimization of effective concentrations, the positive effectors CspC and CspE could be targets for increasing CFE rates and/or yields through overexpression or stabilization of these proteins in chassis strains used for extract preparation, and removal of CspD from the extract source strain could provide similar benefits. The relatively low abundance reported in the literature for CspA and C (with no detection of CspD or E) in a high-yielding commercial CFE kit suggests the potential applicability of these proteins across the cell-free synthetic biology community.[53] Additionally, balancing the nucleic acid interactions of polyamines and cold-shock proteins along with their concentration-dependent effects on CFE productivity could increase the robustness of CFE formulations.[54,79] We predict that effector proteins identified here and in the previous literature could have more significant impacts on the CFE of alternative proteins or under nonstandard reaction conditions. Supplementing chaperones enhances the solubility of aggregation-prone proteins,[82] cold-shock family proteins more significantly impact CFE yields at low temperatures,[79] and several effector proteins were identified through a beta-lactamase expression screen in a different extract background.[83] Future studies should consider these findings in the context of reaction formulation and conditions to better understand the specific CFE system employed and potentially increase protein synthesis capacity.

CONCLUSIONS

Recent studies have partially characterized the contents and behavior of *E. coli* extracts for transcription and translation, but the focus has been either on providing an inventory of proteins or metabolites or on optimizing gene expression.[46,51−54,71] In this work, we sought to assess the impact of extract processing on both the complement of biomolecules present in the extract and the potential for gene expression through the most comprehensive analysis of the *E. coli* extract to date. A key feature was connecting observed changes in the extract proteome and metabolome to differences in CFE activity, especially from σ^{70} promoters. After comparing expression profiles, metabolites, and proteins across differentially processed cell extracts, we observed that the most significant increase in σ^{70} gene expression results from runoff incubation and the associated proteome changes. Supplementing the most significantly depleted proteins into CFE reactions altered expression kinetics, highlighting cold-shock and RNase-related proteins as notable effectors of cell-free protein synthesis. While the *E. coli* extract remains a complex system with significant differences between the well-known model organisms and further differences between research groups using variable methodologies,[44] we believe that this analysis provides significant insights into the behavior and composition of the cell extract within the constraints of our analytical methods. For example, our supplementation assays were limited by the concentration and stability of purified proteins, which are difficult to overcome in CFE reactions that have a defined volume and can be impacted by changes in buffer pH, ionic strength, and other factors.

https://doi.org/10.1021/acssynbio.2c00339
ACS Synth. Biol. 2023, 12, 405−418

Looking forward, insights gained through this study may provide the basis for further investigation into the roles of and interactions between cold-shock family proteins, RNases, and their regulators in CFE from σ^{70} promoters with potential extensions to T7-driven expression. Furthermore, data-driven, systems-level optimization and analysis of cell-free systems will enable greater control and reproducibility of cell-free synthetic biology applications.

MATERIALS AND METHODS

Strains, Plasmids, and Chemicals. Cell extracts were prepared from BL21 Star (DE3) cells originally from Life Technologies. Reporter plasmids included pJBL7004 (T7-MGA, Addgene #136943), pJL1 (T7-sfGFP, Addgene #69496), pJBL7007 (σ^{70}-MGA, Addgene #136946), and pJBL7010 (σ^{70}-sfGFP, Addgene #136942). These plasmids were isolated using the ZymoPURE II Plasmid Maxiprep kit (Zymo Research), ethanol precipitated, and quantified via NanoDrop (Thermo Scientific) prior to use in cell-free reactions. Plasmid templates were normalized to molar concentrations for consistency in reactions. Plasmids for the supplementation experiment were produced by Twist Bioscience in either pJL1 or pETBCS backbones[84] with an added CAT-Strep-linker tag[85] and amplified with Q5 high-fidelity polymerase (NEB) to generate linear expression templates. Primers for linear template generation had the following sequences: 5′-ctgagatacctacagcgtgagc-3′ (forward) and 5′-cgtcactcatggtgatttctcacttg-3′ (reverse). Sequences for each protein are provided in Table S6. All chemicals and reagents were ordered from MilliporeSigma unless otherwise noted.

Cell Extract Preparation. This protocol is based on established methods using acetate[38] or glutamate[46] buffers to wash and resuspend cells prior to lysis. BL21 Star (DE3) cells were isolated from a distinct colony on LB agar plates (10 g/L tryptone, 5 g/L yeast extract, 5 g/L NaCl, and 15 g/L agar) and grown overnight at 37 °C in 75 mL of 2xYTP media (16 g/L tryptone, 10 g/L yeast extract, 5 g/L NaCl, 7 g/L K_2HPO_4, and 3 g/L KH_2PO_4 adjusted to a pH of 7.2 with 5 N KOH). Although 2xYTPG is commonly used for T7-driven CFE, it has been shown that glucose in the culture media can reduce σ^{70}-driven CFE.[46,54] Therefore, we omitted glucose during cell growth to ensure that σ^{70} expression was not inhibited in the cell-free reactions. The following day, 10 L of sterilized 2xYTP with 0.5 mL of Antifoam 204 was inoculated with the overnight culture to an initial OD_{600} of 0.06−0.08 in a BIOSTAT Cplus bioreactor (Sartorius Stedim) set to 600 rpm with airflow at 8 SLPM. Cells were grown at 37 °C to an OD_{600} of 3.0−3.2 (∼3.5 h) prior to centrifugation for 8 min at 6000*g* in 1 L bottles at 4 °C. The resulting pellets were separated into two 50 mL conical tubes each and washed with 20 mL of either S30-Acetate [10 mM Tris base adjusted to a pH of 8.2 with acetic acid, 14 mM magnesium acetate, 60 mM potassium acetate, and 2 mM dithiothreitol (DTT)] or S30-Glutamate (50 mM Tris base, 14 mM magnesium glutamate, 60 mM potassium glutamate, and 2 mM DTT, adjusted to a final pH of 7.7). After resuspension by vortex in 15 s intervals to avoid overheating, the cell suspensions were centrifuged for 2 min at 20,000*g* and 4 °C. The wash, resuspension, and centrifugation were repeated twice more for a total of three washes with each pellet only exposed to either acetate or glutamate buffer. The mass of each washed cell pellet was determined, and then, the pellets were flash frozen in liquid nitrogen prior to storage at −80 °C. Four biological replicates were harvested from unique starting colonies, and the cell pellets were processed into extract on four separate days.

After thawing on ice for 1 h, cell pellets were resuspended with 1 mL of S30 (acetate or glutamate) per gram of biomass by vortexing in 15 s intervals. Cells were lysed with a single pass through an Avestin EmulsiFlex-B15 homogenizer set to 20,000−25,000 psi. Lysate aliquots were collected at this point for analysis, and the remaining volume was transferred to 1.5 mL tubes for 10 min centrifugation at 12,000*g* and 4 °C. The supernatant was recovered and further processed. Extracts without additional processing were centrifuged again for 10 min at 12,000*g* and 4 °C to remove the residual insoluble protein, and the resulting supernatant was flash frozen. Extracts with runoff were incubated at 37 °C for 80 min prior to centrifugation and flash freezing. Dialyzed extracts were transferred to 10 kDa molecular weight cutoff Slide-A-Lyzer cassettes (Thermo Scientific) and dialyzed for 3 h at 4 °C in a 200× volume of buffer−either S30-acetate or Dialysis-G (5 mM Tris base, 14 mM magnesium glutamate, 60 mM potassium glutamate, and 1 mM DTT, with a pH of 8.2 without adjustment). Extracts processed following both steps went through runoff, centrifugation, dialysis, and another centrifugation prior to flash freezing the supernatant. Differences in buffer salt (acetate or glutamate) refer only to extract preparation and processing; the same CFE recipe (using glutamate salts) was used for all reactions.

Cell-Free Gene Expression. CFE reactions were formulated based on the Panox-SP system[33] with 1−20 nM DNA template. These reactions contained 26.7% *E. coli* extract by volume (∼12−15 mg/mL); 57 mM HEPES buffer; 8 mM magnesium glutamate; 10 mM ammonium glutamate; 130 mM potassium glutamate; 1.2 mM adenosine triphosphate; 0.85 mM each of guanosine, uridine, and cytidine triphosphates; 0.034 mg/mL folinic acid; 0.171 mg/mL transfer RNAs; 33.33 mM phosphoenolpyruvate; a 2 mM concentration of each canonical amino acid; 0.40 mM nicotinamide adenine dinucleotide; 0.27 mM coenzyme A; 1 mM putrescine; 1.5 mM spermidine; and 4 mM oxalic acid. In addition to these reagents, purified T7 RNA polymerase (0.10 mg/mL) was added for transcription from T7 promoters, and 100 μM malachite green oxalate was added to observe MGA expression. CFE reactions in quadruplicate were set up on ice in clear-bottom 384-well plates at the 10 μL scale and transferred to a Biotek Synergy H1 plate reader for kinetic measurements of sfGFP (485/520 nm excitation/emission) and MGA (615/650 nm excitation/emission) at 30 °C for 8−20 h with measurements every 5 min sfGFP fluorescence is reported as molecules of equivalent fluorochrome based on standard curves of fluorescein isothiocyanate. Maximum reactions rates were determined by generating a linear regression of fluorescence over every 20 minute window for a given CFE reaction and then obtaining the maximum slope. Maximum rates for each replicate were averaged to achieve a maximum rate for the given condition.

Metabolomics. Cell-free extract samples representing four biological replicates each prepared in eight different conditions were analyzed by GC−MS using previously described methods.[20] Briefly, samples stored at −80 °C prior to analysis were thawed, and following centrifugation at 12,000 rpm at 4 °C for 15 min, an aliquot of 10 μL was transferred to a vial containing 10 μL of sorbitol (1 mg/mL aqueous solution) as an internal standard and then dried under a stream of N_2. Dried samples were dissolved in 250 μL of silylation-grade

https://doi.org/10.1021/acssynbio.2c00339
ACS Synth. Biol. 2023, 12, 405−418

acetonitrile, followed by the addition of 250 μL of *N*-methyl-*N*-(trimethylsilyl)trifluoroacetamide with 1% trimethylchlorosilane (Thermo Scientific, Bellefonte, PA) and heated for 1 h at 70 °C to generate trimethylsilyl derivatives. After 2 days, 1 μL aliquots were injected into an Agilent Technologies 7890A gas chromatograph coupled to a 5975C inert XL mass spectrometer fitted with an RTX-5MS (5% diphenyl/95% dimethyl polysiloxane) 30 m × 250 μm × 0.25 μm film thickness capillary column with a 5 m Integra-Guard column. Gas flow was 1.0 mL per minute, and the injection port was configured for splitless injection. The initial oven temperature was 50 °C with a 2 min hold, followed by a temperature ramp of 20 °C per minute to 325 °C and hold for another 11.5 min. The mass spectrometer was operated in the standard electron impact (70 eV) ionization mode. The injection port, MS transfer line, MS source, and MS quad temperatures were 250, 300, 230, and 150 °C, respectively. A large user-created database and the commercially available Wiley Registry 10th Edition combined with the NIST 14 mass spectral database were used to identify metabolites of interest. Peaks were quantified by using extracted-ion chromatograms rather than total ion current chromatograms, utilizing a key selected ion characteristic *m*/*z* fragment, to minimize co-eluting metabolites. The extracted-ion chromatogram was scaled back to the total ion chromatogram using predetermined scaling factors, and quantification was based on area integration and normalized to the quantity of the internal standard recovered, the volume of the sample processed, the derivatization volume, and the injection volume.

Targeted Metabolite Analysis. 10 μL reactions were run in biological triplicate with 5 nM DNA to observe changes in central metabolites over the course of CFE. Separate samples were quenched at each time point with 10 μL of 10% (w/v) trichloroacetic acid, and precipitated proteins were removed by centrifugation for 10 min at 20,000*g*. The supernatant was transferred to vials, and 5 μL was injected on an Agilent 1260 HPLC system. Metabolites were separated with 5 mM sulfuric acid flowing at 0.6 mL/min on a Rezex ROA-Organic Acid H+ (8%) LC Column (Aminex) at 20 °C. Metabolite concentrations were determined using a refractive index detector or a diode array detector at 210 nm based on the retention time of standard solutions for each compound. Abundance values for all metabolites are provided in Data Set S1, and information for unknown metabolites is provided in Table S1.

Proteomics Sample Preparation. Samples (in biological quadruplicates) spanning different processing steps (crude lysate, no processing, after runoff, after dialysis, and after both runoff and dialysis) for both acetate and glutamate salts were frozen and stored at −80 °C until proteomic analysis. Samples were thawed, diluted 1:1 with 4% SDS (sodium dodecyl sulfate) in Tris−HCl (100 mM at a pH of 8.0), and adjusted to 10 mM DTT (DL-dithiothreitol), followed by heat treatment at 95 °C for 10 min to denature the proteins and reduce the disulfide linkages. The crude protein amount was determined using a NanoDrop One^C Microvolume UV−vis spectrophotometer (Thermo Scientific) by measuring the corrected absorbance at 205 nm. Samples were then adjusted to 30 mM IAA (iodoacetamide) and incubated for 20 min in darkness at room temperature to alkylate/block cysteine residues. Crude protein was then cleaned up using the protein aggregation capture[86] method prior to digestion. Briefly, 250 μg of magnetic beads (1 μm SpeedBead magnetic carboxylate modified particles; GE healthcare UK) were suspended in the same amount of crude protein lysate, and aggregation of proteins onto the beads was induced by the addition of acetonitrile to a final concentration of 70%, followed by a 20 min incubation. The protein bead aggregate was then washed with 1 mL of 100% acetonitrile followed by 1 mL of 70% ethanol. Aggregated proteins were then digested with MS grade trypsin protease (1:75 w/w; Pierce-Thermo Scientific) in Tris−HCl (100 mM, pH 8.0) for 3 h at 37 °C and again overnight at 37 °C. Tryptic peptides were then acidified with formic acid (FA; LC/MS grade) to a final concentration of 0.5% and filtered through a 10 kDa MWCO centrifugal concentrator (Vivaspin500 PES; Sartorius) to remove underdigested proteins. The resulting peptides were again quantified using a NanoDrop One^C.

Reversed-Phase Chromatography and Tandem Mass Spectrometry. Two micrograms of peptides from each sample was analyzed by reversed-phase 1D LC−MS/MS using a Vanquish UHPLC system (Thermo Scientific) coupled to an Orbitrap Q-Exactive Plus mass spectrometer (Thermo Scientific), as previously described.[87] Briefly, peptides were trapped on an in-house developed single frit trapping column (100 μm ID) packed with 6 cm of C_{18} resin (5 μm Kinetex; Phenomenex) and separated by an organic gradient on an in-house pulled nanospray emitter (75 μm ID) packed with 15 cm of C_{18} resin (1.7 μm Kinetex; Phenomenex). Sample loading, trapping, and desalting were performed for 30 min in solvent A (0.1% FA in 5% acetonitrile) at 2 μL/min. For peptide elution and analytical separation, the flow rate was split to achieve 300 nL/min. The gradient was as follows: 0−30% solvent B (0.1% FA in 70% ACN) over 185 min, increase to 0% solvent B over 5 min, and hold for 15 min at 100% solvent A. Each elution was followed by a column wash: 0 to 100% solvent B over 15 min, hold at 100% solvent B for 5 min, decrease to 0% solvent B over 5 min, and final equilibration with 100% solvent A for 15 min before injection of the next sample. The total analysis time was 275 min for each peptide sample, with spectra collected during the first 240 min.

Eluting peptides were measured and sequenced using the Orbitrap Q-Exactive Plus mass spectrometer (operated via Xcalibur v4.2.47, Thermo Scientific) in the data-dependent mode. Full-scan MS spectra were acquired in the range *m*/*z* 300−1500 at a resolution of 70,000 [full width at half-maximum (fwhm)] with an AGC target value of 1×10^6. For fragmentation, the 20 most intense precursor ions were selected for MS/MS with an isolation window set to 1.8 *m*/*z* and dynamic exclusion set to 30 s. HCD fragmentation was performed at a normalized collision energy of 27% with an AGC target value of 1×10^5 and a resolution of 17,500 (fwhm).

Proteomics Data Analysis. The resulting peptide fragmentation spectra were searched against the *E. coli* BL21(DE3) proteome (UniProt downloaded January 2021, 4156 entries) appended with sfGFP sequence and a common protein contaminants database via a target decoy approach using the MS Amanda algorithm (v2.0) integrated in Proteome Discoverer software (version 2.3.0.523, Thermo Scientific). Peptide spectrum matches (PSMs) were required to be at least five amino acids long, fully tryptic with a maximum of two missed cleavages, with a static modification of 57.0214 Da on cysteine residues (carbamidomethylated) and a dynamic modification of 15.9949 Da on methionine residues (oxidized). PSMs and peptides were scored and filtered at a false discovery rate (FDR) of 1% using the IMP-Elutator node in Proteome

https://doi.org/10.1021/acssynbio.2c00339
ACS Synth. Biol. 2023, 12, 405−418

Discoverer. Peptides were quantified by chromatographic area under the curve, and match between runs was enabled by performing a grouped consensus step in Proteome Discoverer on all the samples. Peptides were then mapped to their respective proteins, and their areas were summed to estimate protein-level abundances. Proteins were filtered to retain those with a protein FDR of ≤1%, abundances were $\log_2$ transformed, and distributions were LOESS normalized and median centered in InfernoRDN.[88] The proteome data set was further filtered to retain those proteins that were quantified in at least three samples, and missing values were imputed in Perseus v1.6.14.0[89] to simulate the MS limit of detection. Significant differences in protein abundances between the "no processing" conditions and the "processed" samples were measured by two-tailed Student's *t*-tests at a Benjamini-Hochberg FDR corrected *p*-value of ≤0.05. Hierarchical clustering of significant proteins was performed in JMP Pro14 software using the fast ward method. Annotations were downloaded from UniProtKB and Kyoto Encyclopedia of Genes and Genomes (KEGG). Protein interaction information was downloaded from the STRING database. For identification and quantification of modifications on peptides, PEAKS PTM analysis was performed in PEAKS studio as described previously.[90,91] Plots were generated using R and Python scripts and Cytoscape v3.8.2.

Protein Purification and Supplementation. Proteins identified in Figure S10 were ordered in expression vectors from Twist Bioscience with CAT-Strep-linker tags[85] for affinity purification. All proteins were initially expressed by CFE as described above from linear expression templates with ^{14}C-leucine incorporation[92] to quantify total and soluble yields of each protein (Figure S9). For the initial screen (Figure 5A), proteins with >3.5 μM soluble yield were produced in 250 μL CFE reactions in 50 mL tubes, while proteins with less than 3.5 μM soluble yield were expressed in vivo by BL21(DE3) with a pETBCS plasmid in 10 mL of Overnight Express instant TB autoinduction media for 20 h. Cells were pelleted by centrifugation (resulting in ∼0.2 g of wet biomass) and then lysed by the addition of 1 mL BugBuster Master Mix. Insoluble debris was removed from cell-free reactions and lysed cell cultures by centrifugation at 10,000*g*, and the strep-tagged protein was purified from each supernatant using 30 μL of MagStrep "type3" XT beads 5% suspension (IBA). Eluted proteins were processed using Zeba Micro Spin Desalting Columns (ThermoFisher) with a 7 kDa molecular weight cutoff to exchange the high-salt elution buffer with Dialysis-G used in extract processing (without DTT) to increase compatibility with CFE. Purified proteins were quantified by the Bradford assay (BioRad) and analyzed by SDS-polyacrylamide gel electrophoreses (PAGE) using NuPAGE 4−12% Bis-Tris Protein Gels (ThermoFisher) with MOPS running buffer (Figure S10). All proteins that were soluble after purification and aligned with the expected mass were supplemented into CFE reactions at 20% of the final volume (Figure 5A) using the extract prepared with glutamate buffer, runoff, and dialysis to observe the impact of these proteins on the expression of σ^{70}-sfGFP relative to a negative control of elution buffer processed alongside the proteins using a Zeba desalting column.

Proteins shown in Figure 5A that significantly increased or decreased the rate of σ^{70}-sfGFP expression ($p < 0.05$ by 2-tailed Student's *t*-test) were selected for analysis of concentration-dependent effects. Additionally, Ugd and Nano-Luc luciferase were chosen as native and heterologous proteins to serve as controls for the impact of increasing purified protein concentration in CFE as Ugd resulted in no significant difference in expression. In order to purify larger volumes, all proteins were expressed in vivo from pETBCS plasmids in 50 mL of Overnight Express instant TB autoinduction medium for 20 h. Cells were pelleted by centrifugation (resulting in ∼2.5 g wet biomass) and then lysed by the addition of 5 mL of BugBuster Master Mix. Insoluble debris was removed from the lysates by centrifugation at 10,000*g*, and the strep-tagged protein was purified from each supernatant using 0.5 mL of Strep-TactinXT 4Flow resin (IBA) on BioRad PolyPrep chromatography columns. Due to the poor initial purification of CspE, this protein was expressed in four 250 μL CFE reactions and purified with 0.1 mL of resin to concentrate the protein from these pooled reactions. Elution fractions were pooled and dialyzed in Slide-A-Lyzer dialysis cassettes (Thermo Scientific) with a 3.5 kDa molecular weight cutoff into Dialysis-G without DTT. Purified proteins were quantified by the Bradford assay and analyzed by SDS-PAGE (Figure S13). Proteins were supplemented into CFE reactions at 0.05−4 μM to assess the impact on σ^{70}-sfGFP expression, using Dialysis-G to dilute proteins such that all conditions contained purified protein at 20% of the final reaction volume. Positive effectors CspC and CspE were further supplemented up to 20 μM to observe a plateau in their ability to increase the rate of σ^{70}-sfGFP expression. Supplemented reactions were compared to elution buffer that was dialyzed alongside the proteins into Dialysis-G, and *p*-values were determined by a 2-tailed Student's *t*-test.

■ ASSOCIATED CONTENT

Supporting Information

The Supporting Information is available free of charge at https://pubs.acs.org/doi/10.1021/acssynbio.2c00339.

Kinetic curves showing CFE of sfGFP driven by σ^{70} or T7 promoters in differentially processed extracts; kinetic curves of σ^{70}-sfGFP expression with a range of plasmid expressions; kinetic curves of σ^{70}-MGA expression with a range of plasmid expressions; targeted metabolite expressions in differentially processed extracts; the total count of proteins identified in differentially processed extracts; volcano plots showing classification of proteins depleted during centrifugation after cell lysis; identification of modified proteins in the extract proteome; interaction map of 46 proteins that were significantly depleted in all extracts subjected to runoff incubation and 13 additional proteins identified by STRING analysis; protein expression yields in CFE reactions; SDS-PAGE for proteins purified using Strep-Tactin beads; kinetic curves of σ^{70}-sfGFP expression in screening of proteins supplemented into CFE reactions; cotitration of cold-shock family proteins; unknown metabolites identified in metabolomics data; summary of proteins that were significantly depleted in all extracts subjected to runoff incubation and additional interacting proteins identified by STRING analysis; ranked abundance of cold-shock family proteins in differentially processed extracts; endpoint expression data for supplementation screening; endpoint expression data for the highest concentration conditions of putative effector proteins; and protein sequences used for

https://doi.org/10.1021/acssynbio.2c00339
ACS Synth. Biol. 2023, 12, 405−418

expression in pJL1 and/or pET.BCS plasmids for CFE or in vivo production (PDF)

Metabolomics data (XLSX)

Proteomics data (XLSX)

AUTHOR INFORMATION

Corresponding Authors

Robert L. Hettich − *Biosciences Division, Oak Ridge National Laboratory, Oak Ridge, Tennessee 37831, United States;* orcid.org/0000-0001-7708-786X; Email: hettichrl@ornl.gov

Michael C. Jewett − *Department of Chemical and Biological Engineering, Chemistry of Life Processes Institute, and Center for Synthetic Biology, Northwestern University, Evanston, Illinois 60208, United States; Robert H. Lurie Comprehensive Cancer Center and Simpson Querrey Institute, Northwestern University, Chicago, Illinois 60611, United States;* orcid.org/0000-0003-2948-6211; Email: m-jewett@northwestern.edu

Authors

Blake J. Rasor − *Department of Chemical and Biological Engineering, Chemistry of Life Processes Institute, and Center for Synthetic Biology, Northwestern University, Evanston, Illinois 60208, United States;* orcid.org/0000-0001-6662-341X

Payal Chirania − *Biosciences Division, Oak Ridge National Laboratory, Oak Ridge, Tennessee 37831, United States; Graduate School of Genome Science and Technology, University of Tennessee, Knoxville, Tennessee 37996, United States*

Grant A. Rybnicky − *Chemistry of Life Processes Institute, Center for Synthetic Biology, and Interdisciplinary Biological Sciences Graduate Program, Northwestern University, Evanston, Illinois 60208, United States;* orcid.org/0000-0002-0198-4596

Richard J. Giannone − *Biosciences Division, Oak Ridge National Laboratory, Oak Ridge, Tennessee 37831, United States;* orcid.org/0000-0001-8551-0138

Nancy L. Engle − *Biosciences Division, Oak Ridge National Laboratory, Oak Ridge, Tennessee 37831, United States;* orcid.org/0000-0003-0290-7987

Timothy J. Tschaplinski − *Biosciences Division, Oak Ridge National Laboratory, Oak Ridge, Tennessee 37831, United States*

Ashty S. Karim − *Department of Chemical and Biological Engineering, Chemistry of Life Processes Institute, and Center for Synthetic Biology, Northwestern University, Evanston, Illinois 60208, United States*

Complete contact information is available at: https://pubs.acs.org/10.1021/acssynbio.2c00339

Author Contributions

[V]B.J.R., P.C., and G.A.R. contributed equally to this work. B.J.R., G.A.R., A.S.K., and M.C.J. designed the study. B.J.R. and G.A.R. performed and analyzed cell-free experiments. P.C., R.J.G., and R.L.H. collected and analyzed proteomic data. N.L.E. and T.J.T. collected and analyzed metabolomic data. B.J.R., P.C., G.A.R., A.S.K., R.L.H., and M.C.J. wrote the manuscript. All authors edited and reviewed the manuscript. T.J.T., R.J.G., A.S.K., R.L.H, and M.C.J. supervised the research.

Notes

The authors declare the following competing financial interest(s): M.C.J. has a financial interest in SwiftScale Biologics, Gauntlet Bio, Pearl Bio, Inc., Design Pharmaceutics, and Stemloop Inc. M.C.J.s interests are reviewed and managed by Northwestern University in accordance with their competing interest policies. All other authors declare no competing interests.

All raw mass spectral files (proteomics and metabolomics) used in this study are available at the ProteomeXchange Consortium via the MassIVE repository under the MassIVE accession: MSV000088868. The data can be accessed by opening the MassIVE website (http://massive.ucsd.edu/), logging in using the credentials (username "MSV000088868" and password: "cellfree2022"), and searching for the data set with the accession MSV000088868 in the "MassIVE datasets" tab.

ACKNOWLEDGMENTS

The authors thank Adam Silverman for helpful conversations about experiments and the literature. This work was funded by the U.S. Department of Energy Office of Science, Biological and Environmental Research Division (BER) Genomic Science Program (GSP) under Contract no. DE-SC0018249. B.J.R. was supported by a National Defense Science and Engineering Graduate Fellowship (Award ND-CEN-017-095). G.A.R. was supported by the National Science Graduate Research Fellowship Program under Grant no. DGE-1842165. M.C.J. gratefully acknowledges the David and Lucile Packard Foundation and the Camille Dreyfus Teacher−Scholar Program. This manuscript has been co-authored by UT-Battelle, LLC under Contract no. DE-AC05-00OR22725 with the U.S. Department of Energy.

REFERENCES

(1) Bowie, J. U.; Sherkhanov, S.; Korman, T. P.; Valliere, M. A.; Opgenorth, P. H.; Liu, H. Synthetic Biochemistry: The Bio-inspired Cell-Free Approach to Commodity Chemical Production. *Trends Biotechnol.* **2020**, *38*, 766.

(2) Silverman, A. D.; Karim, A. S.; Jewett, M. C. Cell-free gene expression: an expanded repertoire of applications. *Nat. Rev. Genet.* **2020**, *21*, 151−170.

(3) Carlson, E. D.; Gan, R.; Hodgman, C. E.; Jewett, M. C. Cell-free protein synthesis: applications come of age. *Biotechnol. Adv.* **2012**, *30*, 1185−1194.

(4) Kohler, R. Reception of Eduard Buchner's Discovery of Cell-free Fermentation. *J. Hist. Biol.* **1972**, *5*, 327−353.

(5) Buchner, E. Alkoholische Gährung ohne Hefezellen. *Ber. Dtsch. Chem. Ges.* **1897**, *30*, 117−124.

(6) Nirenberg, M.; Leder, P. RNA Codewords and Protein Synthesis. *Science* **1964**, *145*, 1399−1407.

(7) Nirenberg, M.; Matthaei, J. The Dependence of Cell-free Protein Synthesis in E. Coli Upon Naturally Ocurring or Synthetic Polyribonucleotides. *Proc. Natl. Acad. Sci. U.S.A* **1961**, *47*, 1588−1602.

(8) Zawada, J. F.; Yin, G.; Steiner, A. R.; Yang, J.; Naresh, A.; Roy, S. M.; Gold, D. S.; Heinsohn, H. G.; Murray, C. J. Microscale to manufacturing scale-up of cell-free cytokine production–a new approach for shortening protein production development timelines. *Biotechnol. Bioeng.* **2011**, *108*, 1570−1578.

(9) Martin, R. W.; Majewska, N. I.; Chen, C. X.; Albanetti, T. E.; Jimenez, R. B. C.; Schmelzer, A. E.; Jewett, M. C.; Roy, V. Development of a CHO-Based Cell-Free Platform for Synthesis of Active Monoclonal Antibodies. *ACS Synth. Biol.* **2017**, *6*, 1370−1379.

(10) Stark, J. C.; Jaroentomeechai, T.; Moeller, T. D.; Hershewe, J. M.; Warfel, K. F.; Moricz, B. S.; Martini, A. M.; Dubner, R. C.; Hsu, K. J.; Stevenson, T. C.; Jones, B. D.; DeLisa, M. P.; Jewett, M. C. On-demand biomanufacturing of protective conjugate vaccines. *Sci. Adv.* **2020**, *7*, No. eabe9444.
(11) Hershewe, J.; Kightlinger, W.; Jewett, M. C. Cell-free systems for accelerating glycoprotein expression and biomanufacturing. *J. Ind. Microbiol. Biotechnol.* **2020**, *47*, 977−991.
(12) Hunt, A. C.; Case, J. B.; Park, Y.-J.; Cao, L.; Wu, K.; Walls, A. C.; Liu, Z.; Bowen, J. E.; Yeh, H.-W.; Saini, S.; Helms, L.; Zhao, Y. T.; Hsiang, T.-Y.; Starr, T. N.; Goreshnik, I.; Kozodoy, L.; Carter, L.; Ravichandran, R.; Green, L. B.; Matochko, W. L.; Thomson, C. A.; Vögeli, B.; Krüger, A.; VanBlargan, L. A.; Chen, R. E.; Ying, B.; Bailey, A. L.; Kafai, N. M.; Boyken, S. E.; Ljubetič, A.; Edman, N.; Ueda, G.; Chow, C. M.; Johnson, M.; Addetia, A.; Navarro, M.-J.; Panpradist, N.; Gale, M.; Freedman, B. S.; Bloom, J. D.; Ruohola-Baker, H.; Whelan, S. P. J.; Stewart, L.; Diamond, M. S.; Veesler, D.; Jewett, M. C.; Baker, D. Multivalent designed proteins neutralize SARS-CoV-2 variants of concern and confer protection against infection in mice. *Sci. Transl. Med.* **2022**, *14*, No. eabn1252.
(13) Thavarajah, W.; Silverman, A. D.; Verosloff, M. S.; Kelley-Loughnane, N.; Jewett, M. C.; Lucks, J. B. Point-of-Use Detection of Environmental Fluoride via a Cell-Free Riboswitch-Based Biosensor. *ACS Synth. Biol.* **2020**, *9*, 10−18.
(14) Silverman, A. D.; Akova, U.; Alam, K. K.; Jewett, M. C.; Lucks, J. B. Design and Optimization of a Cell-Free Atrazine Biosensor. *ACS Synth. Biol.* **2020**, *9*, 671−677.
(15) Pardee, K.; Green, A. A.; Ferrante, T.; Cameron, D. E.; DaleyKeyser, A.; Yin, P.; Collins, J. J. Paper-based synthetic gene networks. *Cell* **2014**, *159*, 940−954.
(16) Noireaux, V.; Bar-Ziv, R.; Libchaber, A. Principles of cell-free genetic circuit assembly. *Proc. Natl. Acad. Sci. U.S.A* **2003**, *100*, 12672−12677.
(17) Jung, J. K.; Alam, K. K.; Verosloff, M. S.; Capdevila, D. A.; Desmau, M.; Clauer, P. R.; Lee, J. W.; Nguyen, P. Q.; Pastén, P. A.; Matiasek, S. J.; Gaillard, J. F.; Giedroc, D. P.; Collins, J. J.; Lucks, J. B. Cell-free biosensors for rapid detection of water contaminants. *Nat. Biotechnol.* **2020**, *38*, 1451−1459.
(18) Jung, J. K.; Archuleta, C. M.; Alam, K. K.; Lucks, J. B. Programming cell-free biosensors with DNA strand displacement circuits. *Nat. Chem. Biol.* **2022**, *18*, 385−393.
(19) Thavarajah, W.; Verosloff, M. S.; Jung, J. K.; Alam, K. K.; Miller, J. D.; Jewett, M. C.; Young, S. L.; Lucks, J. B. A primer on emerging field-deployable synthetic biology tools for global water quality monitoring. *npj Clean Water* **2020**, *3*, 18.
(20) Krüger, A.; Mueller, A. P.; Rybnicky, G. A.; Engle, N. L.; Yang, Z. K.; Tschaplinski, T. J.; Simpson, S. D.; Köpke, M.; Jewett, M. C. Development of a clostridia-based cell-free system for prototyping genetic parts and metabolic pathways. *Metab. Eng.* **2020**, *62*, 95.
(21) Kelwick, R.; Webb, A. J.; MacDonald, J. T.; Freemont, P. S. Development of a Bacillus subtilis cell-free transcription-translation system for prototyping regulatory elements. *Metab. Eng.* **2016**, *38*, 370−381.
(22) Sun, Z. Z.; Yeung, E.; Hayes, C. A.; Noireaux, V.; Murray, R. M. Linear DNA for rapid prototyping of synthetic biological circuits in an Escherichia coli based TX-TL cell-free system. *ACS Synth. Biol.* **2014**, *3*, 387−397.
(23) Dudley, Q. M.; Cai, Y.-M.; Kallam, K.; Debreyne, H.; Lopez, J. A. C.; Patron, N. J. Biofoundry-assisted expression and characterisation of plant proteins. *Synth. Biol.* **2021**, *6*, ysab029.
(24) Gan, R.; Cabezas, M. D.; Pan, M.; Zhang, H.; Hu, G.; Clark, L. G.; Jewett, M. C.; Nicol, R. High-Throughput Regulatory Part Prototyping and Analysis by Cell-Free Protein Synthesis and Droplet Microfluidics. *ACS Synth. Biol.* **2022**, *11*, 2108−2120.
(25) Karim, A. S.; Dudley, Q. M.; Juminaga, A.; Yuan, Y.; Crowe, S. A.; Heggestad, J. T.; Garg, S.; Abdalla, T.; Grubbe, W. S.; Rasor, B. J.; Coar, D. N.; Torculas, M.; Krein, M.; Liew, F. E.; Quattlebaum, A.; Jensen, R. O.; Stuart, J. A.; Simpson, S. D.; Köpke, M.; Jewett, M. C. In vitro prototyping and rapid optimization of biosynthetic enzymes for cell design. *Nat. Chem. Biol.* **2020**, *16*, 912−919.
(26) Kelwick, R.; Ricci, L.; Chee, S. M.; Bell, D.; Webb, A. J.; Freemont, P. S. Cell-free prototyping strategies for enhancing the sustainable production of polyhydroxyalkanoates bioplastics. *Synth. Biol.* **2018**, *3*, ysy016.
(27) Khatri, Y.; Hohlman, R. M.; Mendoza, J.; Li, S.; Lowell, A. N.; Asahara, H.; Sherman, D. H. Multicomponent Microscale Biosynthesis of Unnatural Cyanobacterial Indole Alkaloids. *ACS Synth. Biol.* **2020**, *9*, 1349−1360.
(28) Rasor, B. J.; Vögeli, B.; Landwehr, G. M.; Bogart, J. W.; Karim, A. S.; Jewett, M. C. Toward Sustainable, Cell-free Biomanufacturing. *Curr. Opin. Biotechnol.* **2021**, *69*, 136.
(29) Dudley, Q. M.; Karim, A. S.; Nash, C. J.; Jewett, M. C. In vitro prototyping of limonene biosynthesis using cell-free protein synthesis. *Metab. Eng.* **2020**, *61*, 251−260.
(30) Liew, F. E.; Nogle, R.; Abdalla, T.; Rasor, B. J.; Canter, C.; Jensen, R. O.; Wang, L.; Strutz, J.; Chirania, P.; De Tissera, S.; Mueller, A. P.; Ruan, Z.; Gao, A.; Tran, L.; Engle, N. L.; Bromley, J. C.; Daniell, J.; Conrado, R.; Tschaplinski, T. J.; Giannone, R. J.; Hettich, R. L.; Karim, A. S.; Simpson, S. D.; Brown, S. D.; Leang, C.; Jewett, M. C.; Köpke, M. Carbon-negative production of acetone and isopropanol by gas fermentation at industrial pilot scale. *Nat. Biotechnol.* **2022**, *40*, 335−344.
(31) Vögeli, B.; Schulz, L.; Garg, S.; Tarasava, K.; Clomburg, J. M.; Lee, S. H.; Gonnot, A.; Moully, E. H.; Kimmel, B. R.; Tran, L.; Zeleznik, H.; Brown, S. D.; Simpson, S. D.; Mrksich, M.; Karim, A. S.; Gonzalez, R.; Köpke, M.; Jewett, M. C. Cell-free prototyping enables implementation of optimized reverse beta-oxidation pathways in heterotrophic and autotrophic bacteria. *Nat. Commun.* **2022**, *13*, 3058.
(32) Liu, D. V.; Zawada, J. F.; Swartz, J. R. Streamlining Escherichia Coli S30 Extract Preparation for Economical Cell-Free Protein Synthesis. *Biotechnol. Prog.* **2005**, *21*, 460−465.
(33) Jewett, M. C.; Calhoun, K. A.; Voloshin, A.; Wuu, J. J.; Swartz, J. R. An integrated cell-free metabolic platform for protein production and synthetic biology. *Mol. Syst. Biol.* **2008**, *4*, 220.
(34) Jaroentomeechai, T.; Stark, J. C.; Natarajan, A.; Glasscock, C. J.; Yates, L. E.; Hsu, K. J.; Mrksich, M.; Jewett, M. C.; DeLisa, M. P. Single-pot glycoprotein biosynthesis using a cell-free transcription-translation system enriched with glycosylation machinery. *Nat. Commun.* **2018**, *9*, 2686.
(35) Dopp, J. L.; Reuel, N. F. Simple, functional, inexpensive cell extract for in vitro prototyping of proteins with disulfide bonds. *Biochem. Eng. J.* **2020**, *164*, 107790.
(36) Martin, R. W.; Des Soye, B. J.; Kwon, Y. C.; Kay, J.; Davis, R. G.; Thomas, P. M.; Majewska, N. I.; Chen, C. X.; Marcum, R. D.; Weiss, M. G.; Stoddart, A. E.; Amiram, M.; Ranji Charna, A. K.; Patel, J. R.; Isaacs, F. J.; Kelleher, N. L.; Hong, S. H.; Jewett, M. C. Cell-free protein synthesis from genomically recoded bacteria enables multisite incorporation of noncanonical amino acids. *Nat. Commun.* **2018**, *9*, 1203.
(37) Des Soye, B. J.; Gerbasi, V. R.; Thomas, P. M.; Kelleher, N. L.; Jewett, M. C. A Highly Productive, One-Pot Cell-Free Protein Synthesis Platform Based on Genomically Recoded Escherichia coli. *Cell Chem. Biol.* **2019**, *26*, 1743−1754.
(38) Kwon, Y. C.; Jewett, M. C. High-throughput preparation methods of crude extract for robust cell-free protein synthesis. *Sci. Rep.* **2015**, *5*, 8663.
(39) Gregorio, N. E.; Levine, M. Z.; Oza, J. P. A User's Guide to Cell-Free Protein Synthesis. *Methods Protoc.* **2019**, *2*, 24.
(40) Zawada, J. F.; Richter, B.; Huang, E.; Lodes, E.; Shah, A.; Swartz, J. R., *High-Density, Defined Media Culture for the Production of Escherichia coli Cell Extracts*; American Chemical Society, 2003; Vol. *862*.
(41) Levine, M. Z.; So, B.; Mullin, A. C.; Fanter, R.; Dillard, K.; Watts, K. R.; La Frano, M. R.; Oza, J. P. Activation of Energy Metabolism through Growth Media Reformulation Enables a 24-

Hour Workflow for Cell-Free Expression. *ACS Synth. Biol.* **2020**, *9*, 2765−2774.
(42) Jewett, M. C.; Swartz, J. R. Mimicking the Escherichia coli cytoplasmic environment activates long-lived and efficient cell-free protein synthesis. *Biotechnol. Bioeng.* **2004**, *86*, 19−26.
(43) Record, M. T.; Courtenay, E. S.; Cayley, S.; Guttman, H. J. Biophysical compensation mechanisms buffering E. coli protein-nucleic acid interactions against changing environments. *Trends Biochem. Sci.* **1998**, *23*, 190−194.
(44) Cole, S. D.; Miklos, A. E.; Chiao, A. C.; Sun, Z. Z.; Lux, M. W. Methodologies for preparation of prokaryotic extracts for cell-free expression systems. *Synth. Syst. Biotechnol.* **2020**, *5*, 252−267.
(45) Hershewe, J. M.; Warfel, K. F.; Iyer, S. M.; Peruzzi, J. A.; Sullivan, C. J.; Roth, E. W.; DeLisa, M. P.; Kamat, N. P.; Jewett, M. C. Improving cell-free glycoprotein synthesis by characterizing and enriching native membrane vesicles. *Nat. Commun.* **2021**, *12*, 2363.
(46) Silverman, A. D.; Kelley-Loughnane, N.; Lucks, J. B.; Jewett, M. C. Deconstructing Cell-Free Extract Preparation for in Vitro Activation of Transcriptional Genetic Circuitry. *ACS Synth. Biol.* **2019**, *8*, 403−414.
(47) Garamella, J.; Marshall, R.; Rustad, M.; Noireaux, V. The All E. coli TX-TL Toolbox 2.0: A Platform for Cell-Free Synthetic Biology. *ACS Synth. Biol.* **2016**, *5*, 344−355.
(48) Caschera, F.; Noireaux, V. Synthesis of 2.3 mg/ml of protein with an all Escherichia coli cell-free transcription-translation system. *Biochimie* **2014**, *99*, 162−168.
(49) Cai, Q.; Hanson, J. A.; Steiner, A. R.; Tran, C.; Masikat, M. R.; Chen, R.; Zawada, J. F.; Sato, A. K.; Hallam, T. J.; Yin, G. A simplified and robust protocol for immunoglobulin expression in Escherichia coli cell-free protein synthesis systems. *Biotechnol. Prog.* **2015**, *31*, 823−831.
(50) Dopp, J. L.; Jo, Y. R.; Reuel, N. F. Methods to reduce variability in E. Coli-based cell-free protein expression experiments. *Synth. Syst. Biotechnol.* **2019**, *4*, 204−211.
(51) Sridharan, H.; Piorino, F.; Styczynski, M. P. Systems biology-based analysis of cell-free systems. *Curr. Opin. Biotechnol.* **2022**, *75*, 102703.
(52) Foshag, D.; Henrich, E.; Hiller, E.; Schäfer, M.; Kerger, C.; Burger-Kentischer, A.; Diaz-Moreno, I.; García-Mauriño, S. M.; Dötsch, V.; Rupp, S.; Bernhard, F. The E. coli S30 lysate proteome: A prototype for cell-free protein production. *New Biotechnol.* **2018**, *40*, 245−260.
(53) Garenne, D.; Beisel, C. L.; Noireaux, V. Characterization of the all-E. coli transcription-translation system myTXTL by mass spectrometry. *Rapid Commun. Mass Spectrom.* **2019**, *33*, 1036−1048.
(54) Miguez, A. M.; McNerney, M. P.; Styczynski, M. P. Metabolic Profiling of Escherichia coli-Based Cell-Free Expression Systems for Process Optimization. *Ind. Eng. Chem. Res.* **2019**, *58*, 22472−22482.
(55) Contreras-Llano, L. E.; Meyer, C.; Liu, Y.; Sarker, M.; Lim, S.; Longo, M. L.; Tan, C. Holistic engineering of cell-free systems through proteome-reprogramming synthetic circuits. *Nat. Commun.* **2020**, *11*, 3138.
(56) Mohr, B.; Giannone, R. J.; Hettich, R. L.; Doktycz, M. J. Targeted Growth Medium Dropouts Promote Aromatic Compound Synthesis in Crude E. coli Cell-Free Systems. *ACS Synth. Biol.* **2020**, *9*, 2986−2997.
(57) Hurst, G. B.; Asano, K. G.; Doktycz, C. J.; Consoli, E. J.; Doktycz, W. L.; Foster, C. M.; Morrell-Falvey, J. L.; Standaert, R. F.; Doktycz, M. J. Proteomics-Based Tools for Evaluation of Cell-Free Protein Synthesis. *Anal. Chem.* **2017**, *89*, 11443−11451.
(58) Kim, J.; Copeland, C. E.; Padumane, S. R.; Kwon, Y. C. A Crude Extract Preparation and Optimization from a Genomically Engineered Escherichia coli for the Cell-Free Protein Synthesis System: Practical Laboratory Guideline. *Methods Protoc.* **2019**, *2*, 68.
(59) Kim, T. W.; Keum, J. W.; Oh, I. S.; Choi, C. Y.; Park, C. G.; Kim, D. M. Simple procedures for the construction of a robust and cost-effective cell-free protein synthesis system. *J. Biotechnol.* **2006**, *126*, 554−561.
(60) Shrestha, P.; Holland, T. M.; Bundy, B. C. Streamlined extract preparation for Escherichia coli-based cell-free protein synthesis by sonication or bead vortex mixing. *Biotechniques* **2012**, *53*, 163−174.
(61) Yim, S. S.; Johns, N. I.; Park, J.; Gomes, A. L.; McBee, R. M.; Richardson, M.; Ronda, C.; Chen, S. P.; Garenne, D.; Noireaux, V.; Wang, H. H. Multiplex transcriptional characterizations across diverse bacterial species using cell-free systems. *Mol. Syst. Biol.* **2019**, *15*, No. e8875.
(62) Dopp, B. J. L.; Tamiev, D. D.; Reuel, N. F. Cell-free supplement mixtures: Elucidating the history and biochemical utility of additives used to support in vitro protein synthesis in E. coli extract. *Biotechnol. Adv.* **2019**, *37*, 246−258.
(63) Underwood, K. A.; Swartz, J. R.; Puglisi, J. D. Quantitative polysome analysis identifies limitations in bacterial cell-free protein synthesis. *Biotechnol. Bioeng.* **2005**, *91*, 425−435.
(64) Failmezger, J.; Nitschel, R.; Sánchez-Kopper, A.; Kraml, M.; Siemann-Herzberg, M. Site-Specific Cleavage of Ribosomal RNA in Escherichia coli-Based Cell-Free Protein Synthesis Systems. *PLoS One* **2016**, *11*, No. e0168764.
(65) Marshall, R.; Noireaux, V. Quantitative modeling of transcription and translation of an all-E. coli cell-free system. *Sci. Rep.* **2019**, *9*, 11980.
(66) Vezeau, G. E.; Salis, H. M. Tuning Cell-Free Composition Controls the Time Delay, Dynamics, and Productivity of TX-TL Expression. *ACS Synth. Biol.* **2021**, *10*, 2508−2519.
(67) Horvath, N.; Vilkhovoy, M.; Wayman, J. A.; Calhoun, K.; Swartz, J.; Varner, J. D. Toward a genome scale sequence specific dynamic model of cell-free protein synthesis in Escherichia coli. *Metab. Eng. Commun.* **2020**, *10*, No. e00113.
(68) Millard, P.; Enjalbert, B.; Uttenweiler-Joseph, S.; Portais, J. C.; Létisse, F. Control and regulation of acetate overflow in Escherichia coli. *Elife* **2021**, *10*, No. e63661.
(69) Burrington, L. R.; Watts, K. R.; Oza, J. P. Characterizing and Improving Reaction Times for E. coli-Based Cell-Free Protein Synthesis. *ACS Synth. Biol.* **2021**, *10*, 1821−1829.
(70) Bennett, B. D.; Kimball, E. H.; Gao, M.; Osterhout, R.; Van Dien, S. J.; Rabinowitz, J. D. Absolute metabolite concentrations and implied enzyme active site occupancy in Escherichia coli. *Nat. Chem. Biol.* **2009**, *5*, 593−599.
(71) Miguez, A. M.; Zhang, Y.; Piorino, F.; Styczynski, M. P. Metabolic Dynamics in Escherichia coli-Based Cell-Free Systems. *ACS Synth. Biol.* **2021**, *10*, 2252−2265.
(72) Keto-Timonen, R.; Hietala, N.; Palonen, E.; Hakakorpi, A.; Lindström, M.; Korkeala, H. Cold Shock Proteins: A Minireview with Special Emphasis on Csp-family of Enteropathogenic Yersinia. *Front. Microbiol.* **2016**, *7*, 1151.
(73) England, C. G.; Ehlerding, E. B.; Cai, W. NanoLuc: A Small Luciferase Is Brightening Up the Field of Bioluminescence. *Bioconjugate Chem.* **2016**, *27*, 1175−1187.
(74) Chi, S. W.; Jeong, D. G.; Woo, J. R.; Lee, H. S.; Park, B. C.; Kim, B. Y.; Erikson, R. L.; Ryu, S. E.; Kim, S. J. Crystal structure of constitutively monomeric E. coli Hsp33 mutant with chaperone activity. *FEBS Lett.* **2011**, *585*, 664−670.
(75) Wisniewski, J. R.; Rakus, D. Quantitative analysis of the Escherichia coli proteome. *Data Brief* **2014**, *1*, 7−11.
(76) Schmidt, A.; Kochanowski, K.; Vedelaar, S.; Ahrné, E.; Volkmer, B.; Callipo, L.; Knoops, K.; Bauer, M.; Aebersold, R.; Heinemann, M. The quantitative and condition-dependent Escherichia coli proteome. *Nat. Biotechnol.* **2016**, *34*, 104−110.
(77) Yamanaka, K.; Zheng, W.; Crooke, E.; Wang, Y. H.; Inouye, M. CspD, a novel DNA replication inhibitor induced during the stationary phase in Escherichia coli. *Mol. Microbiol.* **2001**, *39*, 1572−1584.
(78) Langklotz, S.; Narberhaus, F. The Escherichia coli replication inhibitor CspD is subject to growth-regulated degradation by the Lon protease. *Mol. Microbiol.* **2011**, *80*, 1313−1325.
(79) Higuchi, K.; Yabuki, T.; Ito, M.; Kigawa, T. Cold shock proteins improve E. coli cell-free synthesis in terms of soluble yields of

https://doi.org/10.1021/acssynbio.2c00339
ACS Synth. Biol. 2023, 12, 405−418

aggregation-prone proteins. *Biotechnol. Bioeng.* **2020**, *117*, 1628−1639.
(80) Hofweber, R.; Horn, G.; Langmann, T.; Balbach, J.; Kremer, W.; Schmitz, G.; Kalbitzer, H. R. The influence of cold shock proteins on transcription and translation studied in cell-free model systems. *FEBS J.* **2005**, *272*, 4691−4702.
(81) Roy, S. M.; Bajad, S.; Green, E.; Heinsohn, H. G. Method For Enhancing Recombinant Protein Production by Cell-Free Proten Expression System.U.S. Patent 9,040,253 B2, 2015.
(82) Niwa, T.; Kanamori, T.; Ueda, T.; Taguchi, H. Global analysis of chaperone effects using a reconstituted cell-free translation system. *Proc. Natl. Acad. Sci. U.S.A.* **2012**, *109*, 8937−8942.
(83) Woodrow, K. A.; Swartz, J. R. A sequential expression system for high-throughput functional genomic analysis. *Proteomics* **2007**, *7*, 3870−3879.
(84) Kay, J. E.; Jewett, M. C. Lysate of engineered Escherichia coli supports high-level conversion of glucose to 2,3-butanediol. *Metab. Eng.* **2015**, *32*, 133−142.
(85) Kightlinger, W.; Duncker, K. E.; Ramesh, A.; Thames, A. H.; Natarajan, A.; Stark, J. C.; Yang, A.; Lin, L.; Mrksich, M.; DeLisa, M. P.; Jewett, M. C. A cell-free biosynthesis platform for modular construction of protein glycosylation pathways. *Nat. Commun.* **2019**, *10*, 5404.
(86) Batth, T. S.; Tollenaere, M. X.; Rüther, P.; Gonzalez-Franquesa, A.; Prabhakar, B. S.; Bekker-Jensen, S.; Deshmukh, A. S.; Olsen, J. V. Protein Aggregation Capture on Microparticles Enables Multipurpose Proteomics Sample Preparation. *Mol. Cell. Proteomics* **2019**, *18*, 1027−1035.
(87) Walker, C.; Ryu, S.; Giannone, R. J.; Garcia, S.; Trinh, C. T., Understanding and Eliminating the Detrimental Effect of Thiamine Deficiency on the Oleaginous Yeast Yarrowia lipolytica. *Appl. Environ. Microbiol.* **2020,** *86* (). DOI: 10.1128/AEM.02299-19
(88) Taverner, T.; Karpievitch, Y. V.; Polpitiya, A. D.; Brown, J. N.; Dabney, A. R.; Anderson, G. A.; Smith, R. D. DanteR: an extensible R-based tool for quantitative analysis of -omics data. *Bioinformatics* **2012**, *28*, 2404−2406.
(89) Tyanova, S.; Temu, T.; Sinitcyn, P.; Carlson, A.; Hein, M. Y.; Geiger, T.; Mann, M.; Cox, J. The Perseus computational platform for comprehensive analysis of (prote)omics data. *Nat. Methods* **2016**, *13*, 731−740.
(90) Han, X.; He, L.; Xin, L.; Shan, B.; Ma, B. PeaksPTM: Mass spectrometry-based identification of peptides with unspecified modifications. *J. Proteome Res.* **2011**, *10*, 2930−2936.
(91) Shrestha, H. K.; Appidi, M. R.; Villalobos Solis, M. I.; Wang, J.; Carper, D. L.; Burdick, L.; Pelletier, D. A.; Doktycz, M. J.; Hettich, R. L.; Abraham, P. E. Metaproteomics reveals insights into microbial structure, interactions, and dynamic regulation in defined communities as they respond to environmental disturbance. *BMC Microbiol.* **2021**, *21*, 308.
(92) Rasor, B. J.; Vogeli, B.; Jewett, M. C.; Karim, A. S., Cell-free Protein Synthesis for High-throuhput Biosynthetic Pathway Prototyping. *Cell-Free Gene Expression*; SpringerNature: 2022; Vol. *2433*.

https://doi.org/10.1021/acssynbio.2c00339
ACS Synth. Biol. 2023, 12, 405−418